

Thermal Lagging in Random Media

Da Yu Tzou*

University of Missouri–Columbia, Columbia, Missouri 65211

and

J. K. Chen†

U.S. Air Force Research Laboratory, Kirtland Air Force Base, Albuquerque, New Mexico 87117

The lagging behavior of heat transport in amorphous materials is studied by the use of temperature formulation along with surface heating. The percolating network is alternatively viewed as the physical mechanism causing delayed responses between the heat flux vector and temperature gradient in transporting heat. Experimental results of microsecond responses in rough carbon samples and submillisecond responses in weakly bonded copper spheres are re-examined with emphasis on the possible thermal lagging. Picosecond anomalous diffusion predicted by the fractal and fracton models are compared for silica aerogels and silicon dioxides. It has been shown that the fractal behavior in space can be interpreted in terms of the lagging behavior in time.

Nomenclature

A	= coefficient, dimensionless
C	= volumetric heat capacity, J/m ³ K
D	= fractal and fracton dimensions, dimensionless
d	= Euclidean dimension in phonon vibration, dimensionless
f	= time function of diffusive temperature, $1/\sqrt{s}$
G	= dimensionless heat intensity
g	= heat intensity per unit area, J/m ²
H	= rate of energy exchange, W/m ³ K
k	= thermal conductivity, W/m K
L	= Laplace transform
m	= exponent of time in temperature; slope in the logarithmic temperature vs time plots, dimensionless
N	= truncating terms in Riemann sum
n	= number of terms in Riemann sum
p	= Laplace transform parameter, dimensionless
q	= heat flux, W/m ²
Re	= real part of the function
T	= temperature, K
t	= time, s
x	= one-dimensional space variable, m
y	= integral variable, s
Z	= ratio of τ_T to τ_q , dimensionless
α	= thermal diffusivity, m ² /s
β	= dimensionless time
δ	= Dirac–delta function
η	= dimensionless heat flux
θ	= dimensionless temperature
λ	= intrinsic length scale, m
ξ_i	= correlation length, m, $i \equiv D, W$
τ_q	= phase lag of the heat-flux vector, s
τ_T	= phase lag of the temperature gradient, s
ω	= vibration frequency of fractons or phonons, 1/s
∇	= gradient operator, 1/m
=	= fracton quantity

Subscripts

D	= diffusion
l	= fractal
n	= fracton
q	= heat flux
R	= surrounding
s	= solid tissue, surface
T	= temperature
W	= wave
0	= initial or reference values

Superscripts

–1	= inverse Laplace transform
–	= quantity in the Laplace transform domain

Introduction

LENGTH scale in heat transport is a central quantity in transition from macroscopic to microscopic phenomena. In the classical theory of diffusion employing Fourier's law, exemplified by the one-dimensional form of the diffusion equation the intrinsic length scale is $x \sim \sqrt{\alpha t}$:

$$\frac{\partial^2 T}{\partial x^2} = \frac{\partial T}{\partial(\alpha t)}, \quad \alpha = \text{const} \quad (1)$$

If the energy carriers are modeled as random walkers traveling in Euclidean (homogeneous) geometry, the mean square distance (x^2) is proportional to the travel time t . For isotropic conductors, the random walkers do not have a preferential direction when they travel among lattices. Consequently, the intrinsic length scale in heat diffusion is the same in all directions. The wave theory in heat conduction described by^{1–3} Eq. (2)

$$\frac{\partial^2 T}{\partial x^2} = \frac{\partial T}{\partial(\alpha t)} + \frac{\partial^2 T}{\partial(Ct)^2}, \quad C = \sqrt{\frac{\alpha}{\tau_q}} \quad (2)$$

contains two length scales in the history of heat propagation.⁴ In relatively long-time responses, like diffusion, the intrinsic length scale is proportional to \sqrt{t} , $\lambda_D = \sqrt{\alpha t}$. In the short-time response, on the other hand, the intrinsic length scale is proportional to t , $\lambda_W = Ct$, with C being the finite speed of heat propagation. At the particular instant of time, denoted by τ_q , when the two length scales merge, $\lambda_D = \lambda_W$ at $t = \tau_q$ gives⁴

$$\tau_q = \alpha/C^2 \quad (3)$$

Received Aug. 21, 1997; revision received Jan. 14, 1998; accepted for publication April 16, 1998. This paper is declared a work of the U.S. Government and is not subject to copyright protection in the United States.

*James C. Dowell Professor, Department of Mechanical and Aerospace Engineering. E-mail: tzou@ecn.missouri.edu.

†Directed Energy Effect Research Branch.

which is the thermal relaxation time derived on the basis of molecular collisions.⁵ Parallel to the mean free path of phonon collisions, physically, τ_q measures the mean free time of phonon collisions in heat transport.

Diffusion and thermal wave models describe macroscopic behavior in heat transport, which are averaged over a physical domain much larger than the intrinsic length scales. As the thermal depth of penetration, or the distance traveled by the random walkers in percolating structures, becomes comparable with the intrinsic length scale at short times, these macroscopic models lose their physical supports in macroscopic averaging and refined mechanisms, reflecting the microstructural behavior needing to be accommodated in the description of heat transport. Typical examples include a variety of nanostructured and metastable materials^{6,7} as well as thermal processing of amorphous materials employing short-pulse lasers. The intrinsic length in the macroscopic Fourier diffusion model, λ_D , and thermal wave model, λ_w , is no longer characteristic for heat transport in percolating networks, and additional effort is needed to model the process in microscale.

Amorphous materials have randomly connected internal structures. The microscopic models assuming periodic lattice structures are not expected to provide accurate descriptions for heat transport in this type of material. The concept of fracton transport has been employed to interpret the dynamic behavior of heat transport in fractal networks.⁸⁻¹² The resulting spectral density of states for the vibrations of the percolating network was obtained in the following form^{8,12,13}:

$$D(\omega) \sim \omega^{D_n-1} \quad (4)$$

with $D_n = (2D_i/d_w - 1)$ defining the fracton dimension, D_i standing for the fractal dimension, and d_w for the random-walk dimension in a percolating network. Equation (4) has an identical form to the Debye density of states characterizing the phonon vibration, $D_{\text{Debye}}(\omega) = \omega^{(d-1)}$, with the fracton dimension D_n in Eq. (4) replaced by d . Such an analogy between the density states in the frequency domain facilitates a unified description for the phonon and fractal network vibrations. The fracton theory describes the fractal network in terms of the characteristic length of disorder, in analogy with the correlation length in the percolating theory.¹⁴ The correlation length refers to the average size of holes or clusters in the network, forming the fundamental cell in transporting heat. For physical domains larger than the correlation length, heat transfer occurs in Euclidean geometry and appears to be homogeneous. For physical domains smaller than the correlation length, anomalous behavior may be present and fractal geometry should be used to describe the process of heat transport.

A clear illustration for the intrinsic transition from Euclidean to fractal geometry was recently given by Goldman et al.¹² Based on the heated-mass concept, the temporal behavior of surface temperature for a sample heated by an instantaneous plane source was shown to be characterized by D_i and D_n dimensions:

$$T(0, t) \sim t^{-m}, \quad m = \frac{D_n(D_i - 2)}{2D_i} \quad (5)$$

For an assembly of weakly bonded copper spheres, approximately 100 μm for the averaged diameter and heated by a nanosecond-pulsed laser, the value of m is ~ 0.2 .¹⁵ For silica aerogels having a correlation length of approximately 20 nm, the value of m decreases to 0.06.¹³ The value of m is 0.5 if the process of heat transport is governed by diffusion. A value of m being smaller than 0.5 implies a much slower rate of time in transporting heat, which results from the aerial closures, clusters, bottlenecks, back ends, and many dead ends existing in amorphous media. These complicated internal structures significantly increase the length of the conduction path, rendering a longer mean-square displacement than that in diffusion.^{12,13}

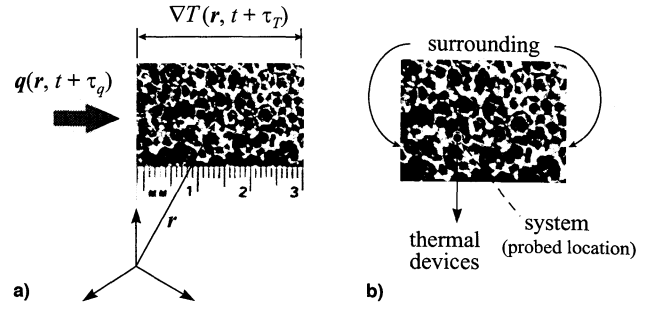


Fig. 1 a) Heat flux flowing through a material volume located at r at time $(t + \tau_q)$ and the temperature gradient established across the material volume at time $(t + \tau_T)$, and b) Definition of system and surrounding in amorphous material.

In this work we study the interrelation between fractal behavior in space and lagging behavior in time for heat transport in amorphous materials. We raise the following question: Can the anomalous behavior of diffusion caused by a long conducting path in amorphous materials be interpreted as the resulting delayed response in time? The physical basis for this viewpoint is illustrated in Fig. 1a, where a duocel aluminum foam with a mass fraction of 6% is displayed. The bright areas are the randomly connected solid (aluminum) tissues and the dark areas are air pores. When heat flux arrives at a representative material volume located at r at time $(t + \tau_q)$, the energy carriers are excited and start to travel along the randomly distributed tissues. Because of the long conducting path that the energy carriers have to pass, however, an instantaneous temperature gradient depicted by Fourier's law, i.e., $\nabla T(r, t) = -q(r, t)/k$, cannot be established across the same material volume. Instead, after arrival of the heat flux at $(t + \tau_q)$, the extra time required for the energy carriers to walk through the long conducting path and the finite time required for the energy carriers to exchange thermal energy with the air pores render the establishment of the temperature gradient at a later time $(t + \tau_T)$. Mathematically, such a lagging behavior between the heat-flux vector and the temperature gradient can be expressed as $\nabla T(r, t + \tau_T) = -q(r, t + \tau_q)/k$, which is the basis for thermal lagging at extremely short times, under extremely low temperatures, and in porous media.¹⁶⁻²⁰ If the lagging behavior is further justified to be suitable for describing heat transport in amorphous media, it may reveal a possible form of the energy equation that reflects the fractal behavior of heat transport in space and time.

On the basis of this observation, we extend the parabolic version of the dual-phase-lag model^{16,19} to study the slowing down of heat transport in relation to the lagging response. It will be shown that the anomalous diffusion is characterized by the ratio of the two phase lags (τ_T/τ_q) in the short-time transient, and the parabolic two-step model indeed preserves several salient features in the existing fractal and fracton models.

Lagging Behavior

In contrast to Fourier's law, where the heat-flux vector and temperature gradient are assumed to be instantaneous, the dual-phase-lag model allows lagging between the heat-flux vector and the temperature gradient.¹⁶⁻²⁰ The parabolic version containing linear effects of τ_T and τ_q takes the following form:

$$q(r, t) + \tau_q \frac{\partial q}{\partial t}(r, t) = -k \nabla T(r, t) - k \tau_T \frac{\partial \nabla T(r, t)}{\partial t} \quad (6)$$

The two phase lags, τ_T and τ_q , are regarded as two intrinsic thermal properties. For the media with $\tau_T < \tau_q$, heat flow is driven by the temperature gradient. For the media with $\tau_q < \tau_T$, on the other hand, heat flow is driven by the heat-flux vector. Such a precedence switch in heat flow is a salient feature in the dual-phase-lag model that cannot be depicted by

Fourier's law (presumed instantaneous response) or a CV-wave model (presumed gradient-precedence response).¹⁸

Equation (8) gives a complicated relation between the heat-flux vector and the temperature gradient. For conductors with a constant thermal conductivity

$$q(r, t) = -ke^{-t/\tau_q} \int_0^t e^{y/\tau_q} \left[\nabla T(r, y) + \tau_T \frac{\partial}{\partial t} \nabla T(r, y) \right] dy \quad (7)$$

In addition to the temperature gradient established across a material volume at time t , the heat-flux vector also depends on the entire history of the temperature gradient (∇T) and its time rate of change $[\partial(\nabla T)/\partial t]$ from 0 to t . Dependence on the time rate of change of the temperature gradient feature distinguishing the dual-phase-lag model from the classical thermal wave model.¹⁹

For examining the possible lagging behavior in a percolating network, a three-dimensional, semi-infinite medium heated by an instantaneous (applied as $t = 0$) plane source (applied at $x = 0$) is considered. Because of the absence of edge effect in planar directions, a one-dimensional analysis is sufficient to study the lagging behavior

$$q(x, t) + \tau_q \frac{\partial q}{\partial t}(x, t) = -k \frac{\partial T}{\partial x}(x, t) - k\tau_T \frac{\partial^2 T}{\partial x \partial t}(x, t) \quad (8)$$

with x axis pointing into the medium from the surface at $x = 0$. The one-dimensional energy equation takes the standard form

$$-\frac{\partial q}{\partial x}(x, t) = C_p \frac{\partial T}{\partial t}(x, t) \quad (9)$$

Anomalous diffusion in random media was studied experimentally by tracking the time history of the surface temperature when subjected to a pulsed surface heating.¹⁵ Because the surface temperature is a major concern, it is intuitive to eliminate the heat flux from Eqs. (8) and (9). The result is called the T representation in the dual-phase-lag model¹⁶⁻¹⁹

$$\frac{\partial^2 T}{\partial x^2} + \tau_T \frac{\partial^3 T}{\partial x^2 \partial t} = \frac{1}{\alpha} \frac{\partial T}{\partial t} + \frac{\tau_q}{\alpha} \frac{\partial^2 T}{\partial t^2} \quad (10)$$

which contains temperature as the sole unknown. Although Eq. (9) is the standard form of the energy equation, clearly, the combined Eq. (10) is more general than the classical diffusion equation [Eq. (1)] and the thermal wave equation [Eq. (2)]. Thermal lagging described by Eq. (8) and, hence, reflected in Eq. (10), contains two additional mechanisms during the short-time transient: the thermalization behavior that is absorbed in the mixed-derivative term and the relaxation behavior that is absorbed in the wave term (the second-order derivative in time).

From a mathematical point of view, two initial conditions are required because of the involvement of the second-order time-derivative in Eq. (10). Assuming a thermal disturbance from a stationary state, in time, the initial conditions are

$$T(x, 0) = T_0, \quad \frac{\partial T}{\partial t}(x, 0) = 0 \quad (11)$$

The laser-pulse duration is usually three to four orders of magnitude smaller than the typical response time in the experiments illustrating the behavior of anomalous diffusion.¹⁵ For rough carbon samples and copper spheres in microscale, for example, the heating pulse was 15 ns, whereas the response time in anomalous diffusion ranges from 0.1 to 1 ms. Because the response time is much larger than the heating duration, it

is suitable to assume a Dirac-delta function in describing the surface heating:

$$q(x = 0, t) = q_s \delta(t) \quad (12a)$$

At a distance away from the heated surface, the thermal disturbance is assumed to vanish

$$T(x, t) \rightarrow T_0 \quad \text{as } x \rightarrow \infty \quad (12b)$$

Note that temperature is the primary unknown in Eq. (10), but heat flux is involved in Eq. (12a). Unlike the case of Fourier diffusion, the complicated integral relation shown by Eq. (7) causes some mathematical difficulties when converting temperature [that satisfies Eq. (10)] to heat flux [that satisfies Eq. (12a)]. A mixed formulation, which approaches Eqs. (8) and (9) simultaneously, was previously adopted to overcome the mathematical difficulty.¹⁹ Alternatively, the present work adheres to the T representation, Eq. (10), in the determination for the lagging temperature. It will be shown that the method of Laplace transform not only removes the intrinsic difficulty residing in Eq. (7), but results in identical characteristics to those in the mixed formulation.

A dimensionless analysis is desirable to identify the dominating parameters in thermal lagging. Introducing

$$\begin{aligned} \theta &= \frac{T - T_0}{T_0}, & \{\eta, \eta_s\} &= \frac{\{q, q_s\}}{T_0 C_p \sqrt{\alpha/\tau_q}} \\ \beta &= \frac{t}{\tau_q}, & \xi &= \frac{x}{\sqrt{\alpha\tau_q}}, & Z &= \frac{\tau_T}{\tau_q} \end{aligned} \quad (13)$$

Equations (10–12) become

$$\frac{\partial^2 \theta}{\partial \xi^2} + Z \frac{\partial^3 \theta}{\partial \xi^2 \partial \beta} = \frac{\partial \theta}{\partial \beta} + \frac{\partial^2 \theta}{\partial \beta^2} \quad (14)$$

$$\theta = 0; \quad \frac{\partial \theta}{\partial \beta} = 0 \quad \text{as } \beta = 0 \quad (15)$$

$$\eta = \eta_s \delta(\beta) \quad \text{at } \xi = 0; \quad \theta(\xi, \beta) \rightarrow 0 \quad \text{as } \xi \rightarrow \infty \quad (16)$$

Although the lagging response depends on both τ_T and τ_q , in general, the ratio of τ_T to τ_q , $Z = \tau_T/\tau_q$ appears as the dominating parameter. This is a general situation in thermal lagging.¹⁹

The Laplace transform solution satisfying Eqs. (14) and (15), and the remote boundary condition in Eq. (16) can be obtained in a straightforward manner

$$\bar{\theta}(\xi, p) = A \exp[-\sqrt{p(1+p)/(1+Zp)}\xi] \quad (17)$$

with A to be determined from the transformed flux condition at $\xi = 0$

$$\bar{\eta} = \eta_s \quad \text{at } \xi = 0 \quad (18)$$

To express Eq. (18) in terms of temperature gradient, consider the nondimensional form of Eq. (6) in the Laplace transform domain:

$$\eta + \frac{\partial \eta}{\partial \beta} = -\frac{\partial \theta}{\partial \xi} - Z \frac{\partial^2 \theta}{\partial \xi \partial \beta} \quad \text{or} \quad \bar{\eta} = -\left(\frac{1+Zp}{1+p}\right) \frac{d\bar{\theta}}{d\xi} \quad (19)$$

Substitution of Eq. (17) into Eq. (19) at $\xi = 0$ results in

$$\bar{\theta}(0, p) = A = \eta_s \sqrt{\frac{1+p}{p(1+Zp)}} \quad (20)$$

which is the transformed surface temperature to be inverted to the physical time domain. In the case of diffusion assuming an instantaneous response between the heat-flux vector and the temperature gradient, $\tau_T = \tau_q$, and implying that $Z = 1$, Eqs. (17) and (20) reduce to

$$\bar{\theta}_D(\xi; p) = \eta_s [\exp(-\sqrt{p\xi}/\sqrt{p})] \quad (21)$$

the Laplace inversion for Eq. (21) is tabulated

$$\theta_D(\xi, \beta) = L^{-1}[\bar{\theta}_D(\xi; p)] = (\eta_s/\sqrt{\pi\beta})e^{-\xi^2/4\beta} \quad (22)$$

which is a well-known result for heat diffusion in a three-dimensional medium heated by an instantaneous surface source.²¹ At the heated surface at $\xi = 0$ the local temperature is inversely proportional to $\sqrt{\beta}$, i.e., $T_D(x, 0) \sim 1/\sqrt{t}$ in terms of the physical variables defined in Eq. (13).

The surface temperature obtained in the Laplace transform domain, Eq. (20), contains three branch points at $p = 0$, -1 , and $-1/Z$. Laplace inversion via the Bromwich contour integration eventually results in an improper integral, which still requires numerical integrations for the physical response in time.²⁰ For this reason, the Riemann-sum approximation for the Laplace inversion is applied to Eq. (20) to obtain the inverse solution^{19,22}

$$\theta(0, \beta) \equiv \frac{e^{4.7}}{\beta} \left[\frac{1}{2} \bar{\theta} \left(0, \frac{4.7}{\beta} \right) + \text{Re} \sum_{n=1}^N \bar{\theta} \left(0, \frac{4.7 + in\pi}{\beta} \right) (-1)^n \right] \quad (23)$$

where the constant 4.7 is selected for faster convergence, and Re denotes the real part of the summation. Equation (23) only involves a summation in the complex domain. The numerical effort involved is comparable with that in the numerical integrations for the Bromwich contour integrals. The Riemann-sum approximation, therefore, is more efficient in this sense. The number of terms in the Riemann sum N increases until a specified Cauchy norm for convergence is satisfied. For results obtained in this work, the Cauchy norm is set to be 10^{-10} .

Ratio of Phase Lags

It is desirable to further study the physical meaning of the phase lags in amorphous materials. As described in Fig. 1b, the probed location for detecting the temperature rise on the solid tissue can be defined as the system. The other portion in the amorphous medium, including the remainder of the randomly connected tissues and air pores, can be defined as the surrounding. In the two-step process describing the thermal energy exchange between the system and the surrounding, the two phase lags can be expressed in terms of the time rate of exchange of thermal energy H between the solid and gaseous phases in the random medium¹⁹

$$\tau_T = \frac{C_s}{H}, \quad \tau_q = \frac{1}{H} \left(\frac{1}{C_R} + \frac{1}{C_s} \right)^{-1} \quad (24a)$$

resulting in

$$Z = \frac{\tau_T}{\tau_q} = 1 + \left(\frac{C_s}{C_R} \right) \quad (24b)$$

Both phase lags depend on the value of H , which is nonzero and remains finite. The ratio between the two, namely the parameter Z , however, depends solely on the ratio of volumetric heat capacities (which can be expressed in terms of the mass fraction), in the amorphous medium.

Results and Discussion

Figure 2 shows the logarithmic plot of surface temperature vs response time for the case of flux-precedence heat flow, Z

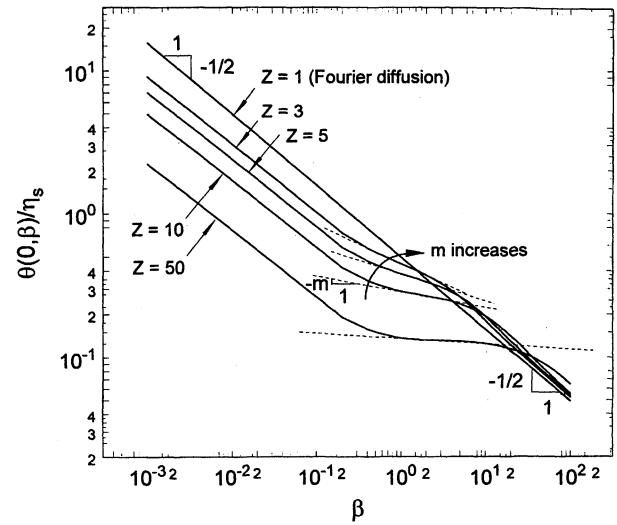


Fig. 2 Logarithmic representation of surface temperature (at $x = 0$) vs time for flux-precedence heat flow ($Z > 1$ or $\tau_T > \tau_q$). The central flatter portion is the region of anomalous diffusion.

$= 1$ (corresponding to the case of diffusion, $\tau_T = \tau_q$) 3, 5, 10, 50 ($Z > 1$). General features of the response curves include 1) the extremely short-time response with $m = 1/2$, 2) the intermediate-time response with $m < 1/2$, and 3) the relatively long-time response with $m = 1/2$. The slope (m) describing the intermediate-time response increases as the value of Z decreases. Because the dual-phase-lag model reduces to the classical diffusion model as the transient time lengthens,¹⁶⁻¹⁹ the case of $m = 1/2$ at stage 3 simply implies retrieval of the Fourier's behavior at longer times. Stage 2 with $m < 1/2$ corresponds to the anomalous region depicted by the fractal and fracton models. The value of m being smaller than one-half ($m < 1/2$) implies a slower rate of heat transport compared with that predicted by Fourier's law, and the rate of heat transport (the value of m) decreases as the value of $Z(\tau_T/\tau_q)$ increases. Stage 1 with $m = 1/2$ at extremely short times deserves special attention. The value of m is the same as that in the long-time response of diffusion at stage 3, which was questioned by Goldman et al.¹² in their study of the picosecond response in silica aerogels, although the experimental result for copper spheres does demonstrate such a special behavior.¹⁵

The long-time (stage 3) and short-time (stage 1) responses with $m = 1/2$ can be justified analytically in the present study. Employing the partial expansion technique,^{19,20} Eq. (20) gives

$$\lim_{\beta \rightarrow 0} \theta(0, \beta) \sim L^{-1}[\lim_{p \rightarrow \infty} \bar{\theta}(0; p)] = \frac{\eta_s}{\sqrt{Z}} L^{-1} \left[\frac{1}{\sqrt{p}} \right] = \frac{\eta_s}{\sqrt{Z\pi}} \cdot \frac{1}{\sqrt{\beta}} \quad (25a)$$

$$\lim_{\beta \rightarrow \infty} \theta(0, \beta) \sim L^{-1}[\lim_{p \rightarrow 0} \bar{\theta}(0; p)] = \eta_s L^{-1} \left[\frac{1}{\sqrt{p}} \right] = \frac{\eta_s}{\sqrt{\pi}} \cdot \frac{1}{\sqrt{\beta}} \quad (25b)$$

[Equations (25a), and (25b) are not the limiting theorem in Laplace transform. The limiting theorem describes the exact behavior at extremely short and long times. The partial expansion technique developed in Ref. 19, on the other hand, describes the fundamental behavior as time approaches zero and infinity.] At extremely short ($\beta \rightarrow 0$) and long ($\beta \rightarrow \infty$) times, the surface temperature clearly has the same behavior, $T \sim t^{-1/2}$. The long-time response shown by Eq. (25b) is independent of the ratio of τ_T to τ_q (Z). The short-time response reflected by Eq. (25a), however, may yield a surface temperature being either lower than the diffusive temperature ($Z > 1$, the flux-precedence type of heat flow) or higher than the diffusive temperature ($Z < 1$, the gradient-precedence type of heat flow).

From the viewpoint of thermal lagging, therefore, the short-time response with a slope of m being one-half¹⁵ is well-supported, although the short-time response is non-Fourier.

Figure 3 shows the experimental result of surface temperature vs time for polished and rough carbon samples obtained by Fournier and Boccara¹⁵ and the response curve obtained by the dual-phase-lag model with $Z = 10$. The early hump at short times with a slope of $-1/3$, Fig. 3a, is preserved in the dual-phase-lag model in the time domain $3 \leq t/\tau_q \leq 100$, Fig. 3b. After $t/\tau_q > 100$, the response curve retrieves that for diffusion with a slope being $-1/2$, like that shown in Fig. 3a for the polished carbon sample at longer times. A precise determination for the values of τ_T and τ_q is difficult because the experimental result of surface temperature was represented in terms of an arbitrary unit (a.u.) in Fig. 3a. Comparison of the characteristic instants of time, as marked in Figs. 3a and 3b, however, suggests that the value of $\tau_q \approx 2.7 \mu\text{s}$ and $\tau_T \approx 27 \mu\text{s}$ (resulting from $Z = 10$) for the rough carbon sample. Figure 4a shows the experimental result of surface temperature vs time for weakly bonded copper spheres obtained by Fournier and Boccara¹⁵ and the response curve obtained by the dual-phase-lag model with $Z = 5$ (Fig. 4b). Note that the copper spheres of a mean diameter being $100 \mu\text{m}$, the characteristic dimension of the interstitial gaseous phase is around $30 \mu\text{m}$. In view of the grain size of coppers ($\approx 1 \mu\text{m}$), thermal energy exchange between the copper spheres and the interstitial gas takes place in microscale. The early- and long-time responses with $m = 1/2$ are preserved in the dual-phase-lag model, referring also to Eqs. (25a) and (25b) for an analytical proof in close form. The anomalous diffusion occurs in $0.2 \leq t/\tau_q \leq 7$, where the slope is reduced by approximately half, reflecting a slowing down of the heat transport rate at the same amount. Comparison of the characteristic instants of time, as marked in Figs. 4a and 4b, reveals that $\tau_q \approx 5 \text{ ms}$ and $\tau_T \approx 25 \text{ ms}$ ($Z = 5$) for weakly bonded copper spheres of a mean diameter $100 \mu\text{m}$.

Figure 5 compares the predicted results of surface temperature vs time for silica aerogels obtained by the fracton model,¹² Fig. 5a, and the dual-phase-lag model with $Z = 50$, Fig. 5b. Again, a qualitative comparison is made here because

of the absence of a physical scale for the surface temperature in Fig. 5a. The short- and long-time behaviors of $m = 1/2$ remain, but the response curve in the anomalous region becomes almost flat, in correspondence with the slope of $m = 0.06$ shown in Fig. 5a. Comparison of the characteristic instants of time, as marked in Figs. 5a and 5b, reveals that $\tau_q \approx 9 \text{ ns}$ and $\tau_T \approx 0.45 \mu\text{s}$ ($Z = 50$) for silica aerogels. Figure 6 shows the corresponding results for silicon dioxide. The results of classical diffusion employing Fourier's law are enclosed for

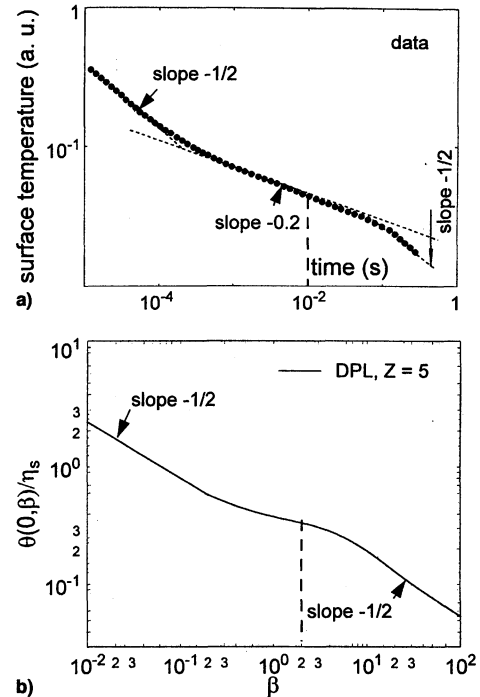


Fig. 4 a) Experimental results of anomalous diffusion in weakly bonded copper spheres, mean diameter $\approx 100 \mu\text{m}$ ¹⁴; and b) corresponding response curve obtained by the dual-phase-lag model with $Z = 5$.

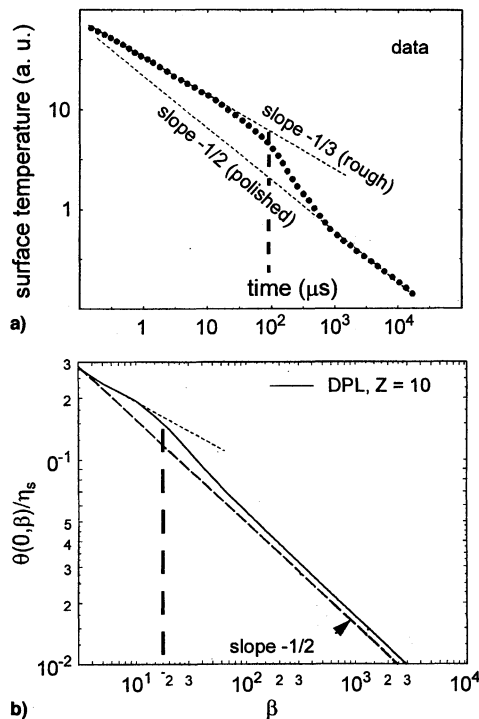


Fig. 3 a) Experimental results of anomalous diffusion in rough carbon samples,¹⁴ and b) corresponding response curve obtained by the dual-phase-lag model with $Z = 10$.

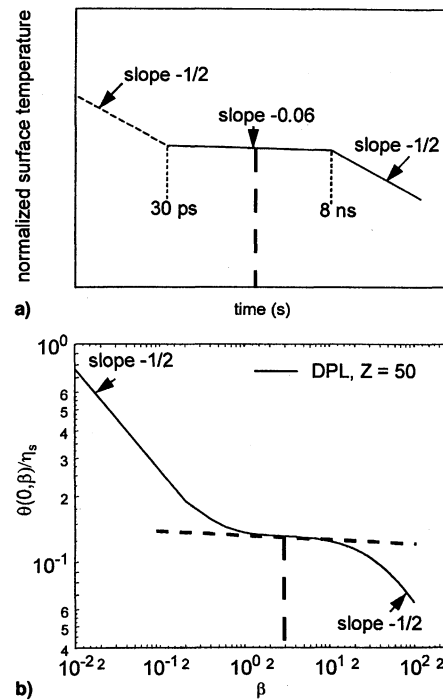


Fig. 5 a) Transient responses predicted by the fractal and fracton models for silica aerogels,¹² and b) corresponding response curve obtained by the dual-phase-lag model with $Z = 50$.

closer comparisons. In the time frame shown in Fig. 6b, the result of classical diffusion has not been recovered yet, but the response curve with thermal lagging becomes parallel to that of diffusion for $t/\tau_q > 30$. This is also the situation shown in Fig. 6a for the fracton model.¹² Comparison of the characteristic instants of time, as marked in Figs. 6a and 6b, reveals that $\tau_q \approx 2$ ps and $\tau_T \approx 10$ ps ($Z = 5$) for silicon dioxide.

A natural question arises at this point: What happens in the anomalous region, particularly in transition from the extremely short-time response? Having exactly the same slope of $m = 1/2$, how does the extremely short-time response differ from the relatively long-time response of diffusion? Figure 7 displays the response curves in linear scales of temperature and time, in correspondence with Fig. 2 in log-scales. Exemplified by the extreme case of $Z = 50$, the response curve with thermal lagging is parallel to that of diffusion at extremely short times, rendering a similar behavior of $T(0, t) \sim t^{-1/2}$, but a signifi-

cantly lower temperature than diffusion. Entering the region of anomalous diffusion at intermediate times, the surface temperature becomes less sensitive with time, resulting in a flatter response curve compared with that of diffusion. Depending on the ratio of τ_T to τ_q (Z), the rate of heat transport in the anomalous region can be many times slower than that of the classical diffusion assuming Fourier's law. The anomalous diffusion prolongs until the response curves with thermal lagging cross over the classical diffusion curve. The lagging temperature becomes higher than the diffusive temperature after the crossover, which is the same behavior discussed by Goldman et al.¹² employing the fracton model for silicon dioxide. The response curve becomes parallel to that of diffusion and, hence, possessing the same behavior of $T(0, t) \sim t^{-1/2}$, at relatively long times.

Figures 2 and 7 show that the classical theory of diffusion may overestimate the transient temperature at extremely short times, but it underestimates the transient temperature at relatively long times. Fourier's law in heat conduction no longer provides a safe bound for the estimate of transient temperature in amorphous materials.

The agreements described in Figs. 3–6 should not be viewed as a result of curve fitting, although the dual-phase-lag model remains phenomenological at this point of development. The two phase lags, τ_T and τ_q , appear in the coefficients of the partial differential equation, Eq. (10), rather than the polynomial used to fit the experimental data. The energy equation must be capable of capturing the essential mechanisms involved in microscale heat transport, yielding distributions that describe the salient features observed in the experiment very well. This is the merit reflected in Figs. 4a and 4b, where all of the salient features at extremely short times ($m = 1/2$), intermediate times ($m < 1/2$), and relatively long times ($m = 1/2$) are absorbed in the distributions obtained by the dual-phase-lag model. The exact, analytical correlation between the dual-phase-lag model and the phonon–electron interaction model and the phonon-scattering model that were derived on the basis of Boltzmann transport equation,^{16,17,19} in addition, provides the physical foundation for describing the microscopic behavior in terms of the resulting delayed response in time. Involving more parameters (τ_T , τ_q , and α) in the dual-phase-lag model (than those in Fourier diffusion and thermal wave models), cannot be viewed as a guaranteed success when describing the experimental phenomena. The high-order, T -wave model that is based on the same phase-lag concept and contains the same number of parameters (τ_T , τ_q , and α) in the thermal lagging,^{17,19} employing the same nondimensional scheme in Eq. (13), for example, does not describe the thermal response resembling the experimental results:

$$\frac{\partial^2 T}{\partial x^2} + \tau_T \frac{\partial^3 T}{\partial x^2 \partial t} = \frac{1}{\alpha} \frac{\partial T}{\partial t} + \frac{\tau_q}{\alpha} \frac{\partial^2 T}{\partial t^2} + \frac{\tau_q^2}{2\alpha} \frac{\partial^3 T}{\partial t^3} \quad (26a)$$

or

$$\frac{\partial^2 \theta}{\partial \xi^2} + Z \frac{\partial^3 \theta}{\partial \xi^2 \partial \beta} = \frac{\partial \theta}{\partial \beta} + \frac{\partial^2 \theta}{\partial \beta^2} + \frac{1}{2} \frac{\partial^3 \theta}{\partial \beta^3} \quad (26b)$$

Under the same initial and boundary conditions, the result obtained from Eq. (26b) with $Z = 50$ is shown in Fig. 8 for illustration. The surface temperature decays with time nonlinearly, even on the logarithmic scale, which completely eliminates all of the salient features shown in Fig. 2.

From a phenomenological point of view, the three stages of energy dissipation reflected by different slopes ($m = 1/2$ at short times, $m < 1/2$ at intermediate times, and $m = 1/2$ again at long times), for bonded copper spheres may be the most representative feature for heat conduction in random media. This is an unusual behavior in heat transport, implying the need to justify its presence from a different approach. Contin-

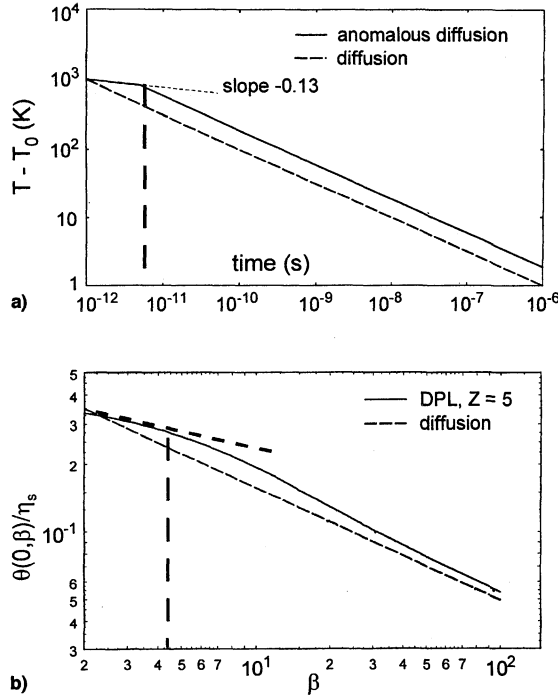


Fig. 6 a) Transient responses predicted by the fractal and fracton models for silicon dioxide,¹² and b) corresponding response curve obtained by the dual-phase-lag model with $Z = 5$.

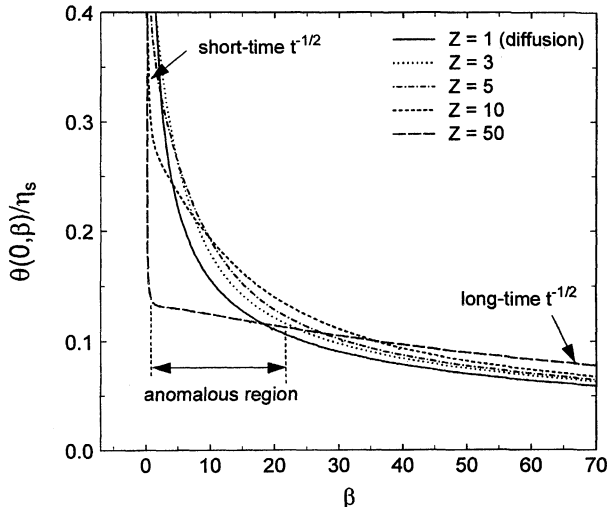


Fig. 7 Response regimes, the short- and long-time responses of $T(0, t) \sim t^{-1/2}$ and anomalous diffusion, of surface temperature on the linear scale.

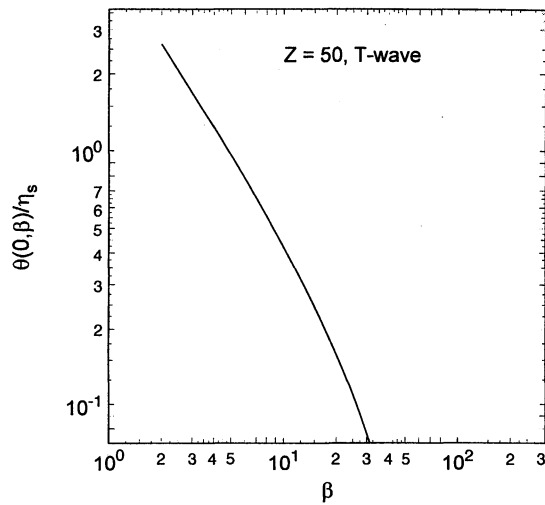


Fig. 8 Lagging behavior resulting from T wave, Eq. (26b), under the same conditions as those in Fig. 2.

using the previous development that employed the mixed formulation in describing heat transport and a volumetric heat source for simulating the energy-absorption rate,¹⁹ the present work confirms the three stages of energy dissipation via the temperature formulation and surface heating, in the same framework of thermal lagging. The temperature-formulation employed in this work is more intuitive, because the experimental phenomena of anomalous diffusion has been studied by the decay of surface temperature with time.

The ratio of two phase lags, $Z = \tau_r/\tau_q$, is again found to be the parameter dominating the heat-transfer rate in the anomalous region. For the flux-precedence type of heat flow with $Z > 1$, which preserves all salient features in the experimental results and the fraction transport model (Figs. 5 and 6), the lagging temperature is lower than the diffusive temperature at extremely short times. The difference between the two increases with the value of Z as shown in Fig. 2. The lower temperature in thermal lagging than that in Fourier diffusion results from the enhancement of thermalization (thermal equilibrium between solid tissues and pores, absorbed in τ_r) during the short-time transient, which is also a salient feature in the picosecond phonon-electron interaction in metals. Entering the anomalous region at intermediate times, the representative slope of the response curve becomes less than one-half ($m < 1/2$), reflecting a slower rate of heat transport in the anomalous region. The representative slope in this region decreases as the value of Z increases. Retrieval of the classical diffusion behavior occurs at relatively long times, after the response curve with thermal lagging crosses over the diffusion curve. Retrieval time for the Fourier's behavior increases with the ratio of τ_r to τ_q (Z), as described in Figs. 2 and 7.

The diffusion-like behavior at early times, $T(0, t) \sim t^{-1/2}$, deserves special attention, as shown in Fig. 2 (analysis) and Fig. 4a (experiment). Although it possesses the same type of temporal behavior as that in diffusion, evidenced by Eqs. (25a), and (25b), the corresponding lagging temperature may be significantly lower than the temperature predicted by Fourier's law. The lagging behavior at extremely short times, therefore, should not be confused with the classical behavior of diffusion. Note, however, that the early-time, $t^{-1/2}$ behavior is withdrawn on the basis of the parabolic dual-phase-lag model in this work. Should the high-order effect of thermal relaxation be found important,^{17,19} the T wave may be activated at extremely short times and the diffusion-like behavior ceases.

In anomalous diffusion the exponent m in Eq. (5) is a constant depending on the fractal and fracton dimensions of the random network. From the viewpoint of thermal lagging, however, the value of m continuously varies in the time-history of temperature. The plateau existing at intermediate times in Fig.

2 does possess a more uniform value of m , which is the regime resembling the anomalous region of heat diffusion described by the fractal and fracton models. It is highly desirable to have an analytical relation between the slope m and the value of Z , for the purpose of characterization. Because of the absence of a closed form solution for the Laplace inversion of Eq. (20), such a relation is difficult to obtain in the present approach. Expanding Eq. (20) in a power series and inverting the result term by term, yields

$$\theta(\xi = 0, \beta) = \left(\frac{1}{\sqrt{Z}}\right) \frac{1}{\sqrt{\beta}} + \left(\frac{Z-1}{Z\sqrt{Z\pi}}\right) \sqrt{\beta} + \left(\frac{3-2Z-Z^2}{6Z^2\sqrt{Z\pi}}\right) \beta^{3/2} + O(\beta^{5/2}) \quad (27)$$

In Eq. (27) the $1/\sqrt{\beta}$ behavior at extremely short times is obvious as $\beta \rightarrow 0$. Anomalous diffusion developed at intermediate times (including the slope m in Fig. 2), however, seems to be a combined result of all the high-order terms in β . Determining an analytical expression relating the slope m to the phase-lag-ratio Z is definitely an important task in future development.

The flux-precedence type of heat flow with $Z > 1$ is emphasized in this work because it gives compatible results with the existing experiments and fractal and fracton models for heat transport in amorphous materials. The gradient-precedence type of heat flow with $Z < 1$ produces a similar behavior in the anomalous region, except that the lagging temperature becomes higher than the diffusion temperature at short-times and lower than the diffusion temperature at relatively long times, a reversed situation to that shown in Fig. 2. A detailed analysis for the gradient-precedence type of heat flow will be postponed until the experimental result supporting this type of behavior becomes available.

There are two major tasks in modeling heat transport in amorphous or random media. The first task is development of new models that reflect the essential mechanisms. The phase-lag concept, the fractal and fracton models,⁸⁻¹² and the general microscopic phonon radiative transport employing the solution to the Boltzmann transport equation²³ are typical examples in this category. They compliment each other despite having intrinsic differences in their fundamental approaches. The thermal wave phenomenon described by the relaxation behavior (τ_q effect) in the dual-phase-lag model, for example, was derived as an acoustically thick limit from the phonon radiative transport equation.^{24,25} The second task is the determination of thermal properties in amorphous solids,^{10,26} including thermal conductivity above the plateau region in its temperature-dependent variations. Although the dual-phase-lag model has been shown to capture several salient features in anomalous diffusion, determination of thermal properties in random media is a prerogative to both the fractal and phonon radiative transport models.

Conclusions

Interpreting anomalous diffusion in terms of the phase-lag concept is one of the ongoing efforts that establish the consistent framework of thermal lagging for a more unified treatment in microscale heat transport. Indeed, different microstructure would result in different physical mechanisms in transporting heat. Detailed modeling following the microstructure, therefore, would be expected to vary in a wide spectrum, covering the Boltzmann transport equation for the molecular distribution function, the microscopic two-step process for phonon-electron interactions, and the fractal and fracton models for accommodating the random structure in amorphous materials.

The phase-lag concept, on the other hand, focuses attention on the delayed response in time that results from the complicated microstructure. Different microstructure results in differ-

ent time delays in transporting heat, which has been described by the two phase lags (τ_r and τ_d) in the dual-phase-lag model. Coincidences with the experimental results, including the $t^{1/2}$ behavior at short times and the slower rate of heat transport at intermediate times (anomalous diffusion), shed light on the further applications of the phase-lag concept to characterize the random medium.

References

- ¹Cattaneo, C., "A Form of Heat Conduction Equation Which Eliminates the Paradox of Instantaneous Propagation," *Compte Rendus*, Vol. 247, 1958, pp. 431–433.
- ²Vernotte, P., "Les Paradoxes de la Théorie Continue de L'équation de la Chaleur," *Compte Rendus*, Vol. 246, 1958, pp. 3154, 3155.
- ³Vernotte, P., "Some Possible Complications in the Phenomena of Thermal Conduction," *Compte Rendus*, Vol. 252, 1961, pp. 2190, 2191.
- ⁴Tzou, D. Y., "An Engineering Assessment to the Relaxation Time in Thermal Wave Propagation," *International Journal of Heat and Mass Transfer*, Vol. 36, 1993, pp. 1845–1851.
- ⁵Chester, M., "Second Sound in Solid," *Physical Review*, Vol. 131, 1963, pp. 2013–2015.
- ⁶Hadjipanyayis, G. C., and Siegel, R. W., *Nanophase Materials: Synthesis, Properties, and Applications*, Kluwer, Dordrecht, The Netherlands, 1994.
- ⁷von der Linde, D., "Ultrashort Interactions in Solids," *Ultrashort Laser Pulses: Generation and Applications*, 2nd ed., edited by W. Kaiser, Springer-Verlag, Heidelberg, 1993, pp. 113–182.
- ⁸Alexander, S., and Orbach, R., "Density of States on Fractals: Fractons," *Journal of Physique Letters*, Vol. 43, 1982, pp. 625–631.
- ⁹Alexander, S., Laermans, C., Orbach, R., and Rosenberg, H. M., "Fracton Interpretation of Vibrational Properties of Cross-Linked Polymers, Glasses, and Irradiated Quartz," *Physical Review B: Solid State*, Vol. 28, 1983, pp. 4615–4619.
- ¹⁰Jagannathan, A., Orbach, R., and Entin-Wohlman, O., "Thermal Conductivity of Amorphous Materials Above the Plateau," *Physical Review B: Solid State*, Vol. 39, 1989, pp. 13,465–13,477.
- ¹¹de Oliveira, J. E., Page, J. N., and Rosenberg, H. M., "Heat Transport by Fracton Hopping in Amorphous Materials," *Physical Review Letters*, Vol. 62, 1989, pp. 780–783.
- ¹²Goldman, C. H., Norris, P. M., and Tien, C. L., "Picosecond Energy Transport by Fractons in Amorphous Materials," *ASME/JSME Thermal Engineering Conference*, Vol. 1, 1995, pp. 467–473.
- ¹³Gefen, Y., Aharony, A., and Alexander, S., "Anomalous Diffusion on Percolating Clusters," *Physical Review Letters*, Vol. 50, 1983, pp. 77–80.
- ¹⁴Havlin, S., and Bunde, A., "Percolation II," *Fractals and Disordered Systems*, edited by A. Bunde and S. Havlin, Springer-Verlag, New York, 1991, pp. 97–150.
- ¹⁵Fournier, D., and Boccara, A. C., "Heterogeneous Media and Rough Surfaces: A Fractal Approach for Heat Diffusion Studies," *Physica (A)*, Vol. 157, 1989, pp. 587–592.
- ¹⁶Tzou, D. Y., "A Unified Field Theory for Heat Conduction from Macro- to Micro-Scale," *Journal of Heat Transfer*, Vol. 117, 1995, pp. 8–16.
- ¹⁷Tzou, D. Y., "The Generalized Lagging Response in Small-Scale and High-Rate Heating," *International Journal of Heat and Mass Transfer*, Vol. 38, 1995, pp. 3231–3240.
- ¹⁸Tzou, D. Y., "Experimental Support for the Lagging Behavior in Heat Propagation," *Journal of Thermophysics and Heat Transfer*, Vol. 9, No. 4, 1995, pp. 686–693.
- ¹⁹Tzou, D. Y., *Macro- to Micro-Scale Heat Transfer: The Lagging Behavior*, Taylor and Francis, Washington, DC, 1997.
- ²⁰Tzou, D. Y., and Zhang, Y. S., "An Analytical Study on the Fast-Transient Process in Small Scales," *International Journal of Engineering Science*, Vol. 33, 1995, pp. 1449–1463.
- ²¹Carslow, H. S., and Jaeger, J. C., *Conduction of Heat in Solids*, Oxford Univ. Press, Oxford, England, UK, 1959.
- ²²Chiffelle, R., "On the Wave Behavior and Rate Effect of Thermal and Thermomechanical Waves," M.S. Thesis, Univ. of New Mexico, Albuquerque, NM, 1994.
- ²³Love, A., and Anderson, P. W., "Estimate of Phonon Thermal Transport in Amorphous Materials Above 50K," *Physical Review*, Vol. 42(B), 1990, pp. 1845–1847.
- ²⁴Majumdar, A., "Microscale Heat Conduction in Dielectric Thin Films," *Journal of Heat Transfer*, Vol. 115, 1993, pp. 7–16.
- ²⁵Joshi and Majumdar, "Transient Ballistic and Diffusive Phonon Heat Transport in Thin Films," *Journal of Applied Physics*, Vol. 74, 1993, pp. 31–39.
- ²⁶Sheng and Zhou, "Heat Conductivity of Amorphous Solids: Simulation Results on Model Structures," *Science*, Vol. 253, 1991, pp. 539–542.